

Recoil-Ion Momentum Distributions for Single and Double Ionization of Helium in Strong Laser Fields

Th. Weber,¹ M. Weckenbrock,¹ A. Staudte,¹ L. Spielberger,¹ O. Jagutzki,¹ V. Mergel,¹ F. Afaneh,¹ G. Urbasch,² M. Vollmer,² H. Giessen,² and R. Dörner^{1,*}

¹*Institut für Kernphysik, Universität Frankfurt, D-60486 Frankfurt, Germany*

²*Fachbereich Physik, Philipps-Universität, Renthof 5, D-35032 Marburg, Germany*

(Received 20 August 1999)

We have measured the momentum distributions of singly and doubly charged helium ions created in the focus of 220 fs, 800 nm laser pulses at intensities of $(2.9\text{--}6.6) \times 10^{14}$ W/cm². All ions are emitted strongly aligned along the direction of polarization of the light. We find the typical momenta of the He²⁺ ions to be 5–10 times larger than those of the He¹⁺ ions and a two peak structure at the highest intensity.

PACS numbers: 32.80.Rm, 31.90.+s, 32.80.Fb

Today, optical fields, which are strong enough to yield 100% probability for singly ionizing helium and other atoms, are routinely accessible in the focus of femtosecond laser pulses. At such high fields, a surprisingly high probability has been found for ionizing even two electrons from helium and other rare gas atoms (see, e.g., [1,2]). The magnitude and field dependence of the He²⁺ ion yield clearly proves that this process relies almost completely on electron-electron correlation and cannot be explained in an independent electron picture. The mechanisms responsible for this two electron transition, however, are a matter of controversy [1–13].

All experimental studies and most of the theoretical work on the double ionization of isolated helium atoms in strong laser fields so far considered only the total ion yield as a function of the laser field strength or polarization. In this Letter, we report on the first differential measurements for the helium double ionization process. Using the well-established technique of cold target recoil-ion momentum spectroscopy (COLTRIMS) [14,15], we have measured the recoil-ion momentum distributions of the He¹⁺ and He²⁺ ions. Such differential ion yields provide more detailed insight into the dynamics of the ionization process and provide a much improved testing ground for the different theoretical models in the discussion.

With the first observation of an enhanced He²⁺ ion yield, Fittinghoff and co-workers [1] suggested that the second electron could be shaken-off by a nonadiabatic change of the potential caused by the emission of the first electron [1], similar to the shakeoff mechanism in high-energy single-photon induced double ionization (see e.g., [16]). In the same analogy to single-photon double ionization, an electron-electron correlation process inside the atom, termed TS1, seems possible [5,16]. Shakeoff and TS1 would take place in a time interval short compared to a single optical cycle.

Alternatively, Corkum [3] suggested that the first electron which is freed by tunneling through the potential barrier of the joint ionic and optical potential and accelerated by the laser field is, in half of the cases, being driven back

to its parent ion. There it can be either elastically scattered, emit higher order radiation, or ionize the second electron in an (*e*, 2*e*) collision [3,7,8,10–12]. In this so-called “rescattering model” there is a time delay of 0.5–1 optical cycles [8] between the emission of the two electrons.

Recently, Becker and Faisal achieved very good agreement for the observed double ionization yields [6,17] with an elaborate *S*-matrix calculation. This theory includes short-time electron correlation (TS1) and the rescattering mechanism as well; both are represented by the same Feynman diagram. It does not include the shake process.

The experimental details of COLTRIMS can be found elsewhere (see [14,15] for reviews); the setup used here was similar to the one used in [18]. In brief, the linearly polarized light of a titanium sapphire laser (Spectra-Physics Spitfire) at 800 nm, with a pulse width of 220 fsec, and a repetition rate of 1 kHz was focused by a 5 cm lens onto a precooled (30 K) supersonic He gas jet target. The focal waist was about 7 μm. The peak laser power was determined by fitting our He¹⁺ ion yields, measured over 5 orders of magnitude as a function of the integral laser power to ion yield calculations of Becker and Faisal (adapted to the present conditions from [6]). We estimate the accuracy of this calibration to be approximately 15%. The result is supported by our measured ratios of the He²⁺/He¹⁺ rate of 0.036%, 0.049%, and 0.085% at intensities of 2.9×10^{14} , 3.8×10^{14} , and 6.6×10^{14} W/cm² [2,6]. The background pressure in the scattering chamber was below 2×10^{-10} mbar; the local He pressure in the gas jet was between 2×10^{-5} and 2×10^{-8} mbar. At 2.9×10^{14} W/cm², ⁴He was used while, for the higher intensities (lower pressure), ³He was used to avoid contamination of the ⁴He²⁺ signal by H₂¹⁺ ions from the residual gas.

The ions created in the focal volume were guided by a homogeneous electric field of about 1 V/cm followed by a drift region onto a position sensitive channel plate with a Roentdek delay-line readout (position resolution <80 μm). From the position of impact and the measured time-of-flight, the recoil-ion charge state and momentum

vector can be deduced. By adjusting the target pressure, a rate of <0.1 ions per laser shot was chosen in order to avoid space charge effects which is crucial given the ion energies in the meV range.

For single ionization (Fig. 1) we find a momentum distribution of the recoiling ions which is strongly aligned along the direction of the electric field vector ϵ of the light. The width of the distribution in the direction of the electric field vector of the light increases with increasing laser power (Fig. 1b). The very narrow He^{1+} momentum distributions are measured simultaneously with the He^{2+} distributions discussed below. They illustrate directly that the problem of possible momentum blurring due to space charge has been successfully avoided. We argue that the ionic momentum distributions are mainly a mirror image of the electron momentum distributions. For single ionization by single-photon absorption with synchrotron radiation (see e.g., [19]) or in the so-called multiphoton regime of strong field ionization, the equivalence of electron and ion momentum distributions is a trivial consequence of momentum conservation, since the momentum of the incoming photon is negligible on the scale discussed here (one 800 nm photon has a momentum of 8×10^{-4} a.u.). In the tunneling regime investigated here, the ion and the electron are accelerated by the laser field. The singly charged ion and the electron experience the opposite acceleration and, hence, opposite momentum transfer from the optical field. Only if the electron can escape the focus during the pulse duration, significant net momentum is transferred to the electron-ion system. Under the conditions of the present experiment, the motion of the electrons during the pulse is small compared to the focal size (1 a.u. corresponds to $0.22 \mu\text{m}$ per 100 fsec).

Figure 2 shows the measured momentum distributions of the He^{2+} ions for intensities of 2.9×10^{14} (a), 3.8×10^{14} (b) and $6.6 \times 10^{14} \text{ W/cm}^2$ (c). The horizontal axis is the ion momentum in the direction of the polarization axis; the vertical axis shows the momentum in the direction of

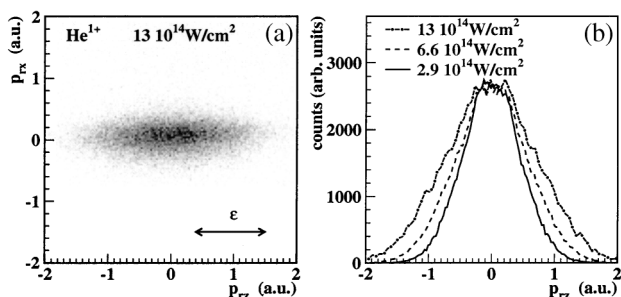


FIG. 1. Momentum distribution of He^{1+} ions created in the focus of a 220 fs, 800 nm laser pulse at peak intensities of $(2.9\text{--}13) \times 10^{14} \text{ W/cm}^2$ and linear polarization. (a) The horizontal axis shows the momentum component along the electric field vector (p_{zr}); the vertical axis is the momentum component in the direction of the light propagation (p_{xr}). The distribution is integrated over p_{yr} . (b) He^{1+} momentum distribution along the electric field vector for different peak intensities as indicated in the figure.

the photon propagation. The distributions are rotational symmetric around the horizontal axis. A projection of Fig. 2 onto the horizontal and vertical axes is shown in Fig. 3. The scattered background in Figs. 2(a) and 3(d) results from H_2^+ ions from the thermal (6.5 a.u. FWHM) hydrogen background in the scattering chamber. For a sequential process, one expects the momentum distributions

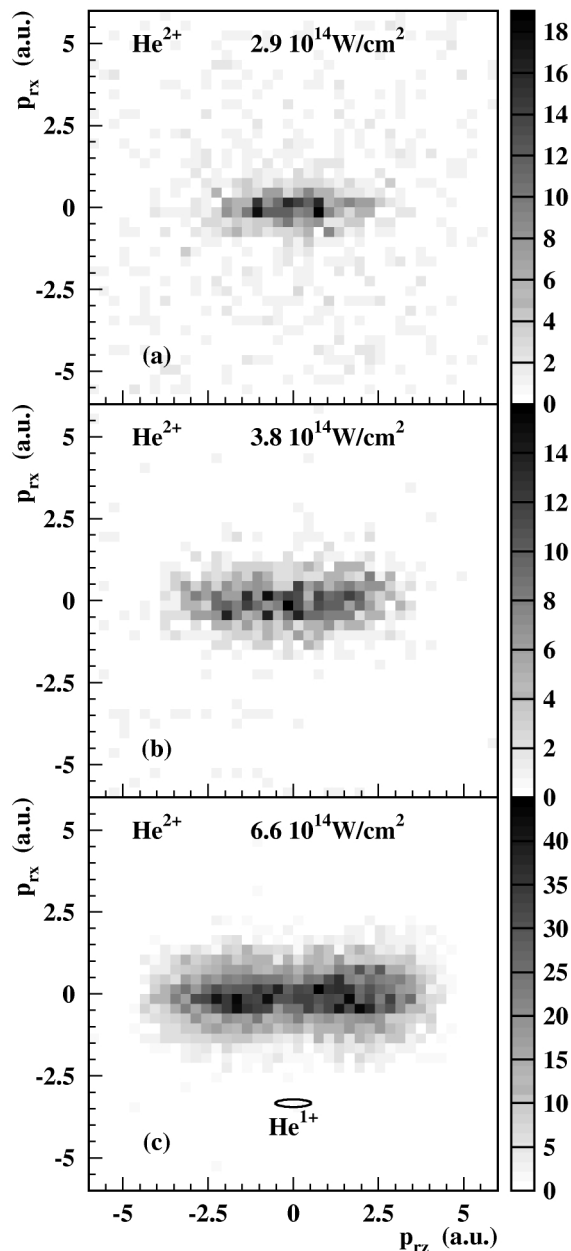


FIG. 2. Momentum distribution of He^{2+} ions created in the focus of a 220 fs, 800 nm laser pulse at peak intensities of 2.9×10^{14} (a), 3.8×10^{14} (b), and $6.6 \times 10^{14} \text{ W/cm}^2$ (c) and linear polarization. The horizontal axis shows the momentum component along the electric field vector (p_{zr}); the vertical axis is the momentum component in the direction of the light propagation (p_{xr}). The distribution is integrated over p_{yr} . The grey value indicates the differential ion yield on a linear scale. The small ellipse in (c) labeled He^{1+} shows the distribution of the half-width of the He^{1+} for comparison.

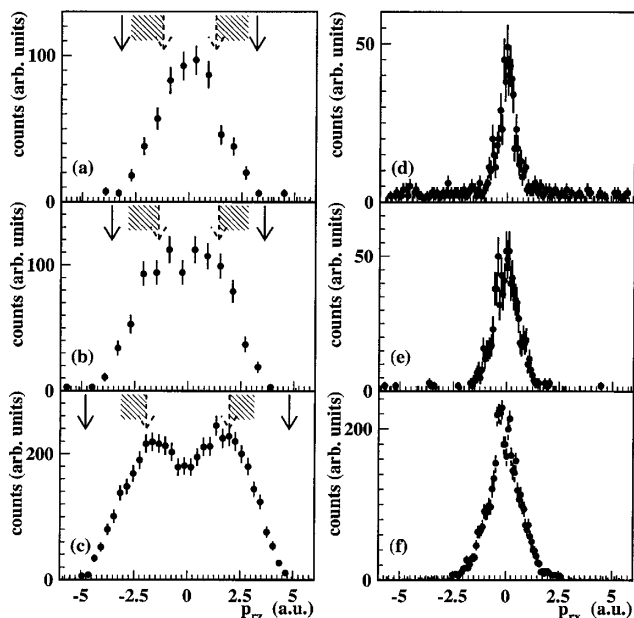


FIG. 3. Projections of Fig. 2 onto the horizontal (a)–(c) and vertical (d)–(f) axes, i.e., (a)–(c) distribution of He^{2+} ion momenta in the direction of the polarization integrated of the two momentum components perpendicular to the polarization. The full arrows indicate a momentum of $2\sqrt{4U_p}$ which is the upper bound if the two electrons are liberated in a time interval short compared to the optical cycle, the dashed arrows indicate the momenta in a rescattering model without momentum transfer in the $(e, 2e)$ collision [Eq. (1)], and the hatched area is an estimate in the rescattering model with momentum transfer (see text). The peak intensities are 2.9×10^{14} W/cm² [(a) and (d)], 3.8×10^{14} W/cm² [(b) and (e)], and 6.6×10^{14} W/cm² [(c) and (f)].

for double ionization to be similar to the distribution for single ionization folded with itself. Thus the very different size of the momenta for single and double ionization (see small ellipse in Fig. 2c) illustrates directly that double ionization does not proceed via sequential single electron processes and, hence, cannot be described by an independent electron approach.

In the following, we will first outline the conclusions which can be drawn from the He^{2+} momentum distribution on the correlated electron momentum distributions. Then we discuss the mechanisms how the ions might receive their momenta. Finally, we relate this to the rescattering and the simultaneous shakeoff/TS1 model.

Based on the same argument outlined above for single ionization, the He^{2+} momentum (p_r) distribution is mainly a mirror image of the distribution of the sum of the vector momenta of the two ejected electrons [$p_r \approx -(p_1 + p_2)$]. Thus the very broad momentum distribution of the He^{2+} ions implies also that the electrons from double ionization have much higher kinetic energy than those from single ionization. The mean recoil-ion energies are 11, 7.2, and 6.7 meV at 2.9×10^{14} , 3.6×10^{14} , and 6.6×10^{14} W/cm² (for single ionization 10 meV recoil-ion energy corresponds to 73 eV electron energy). The broad distribution and, in particular, the minimum at

momentum zero at the highest intensity indicate also that the Wannier configuration of two electrons having equal energy and being emitted back to back ($p_1 = -p_2$) is not a significant contribution to the total cross section. This configuration is allowed by parity conservation for the absorption of an even number of photons (see [20,21]). It would lead to a peak at $p_r = 0$ which is clearly not seen in the data. In contrary, we find contributions up to a momentum of $p_r = 2\sqrt{4U_p}$, where U_p is the ponderomotive energy, i.e., the mean quiver energy of a free electron in the photon field ($U_p = 17.3, 21.5,$ and 39.4 eV at 2.9×10^{14} , 3.6×10^{14} , and 6.6×10^{14} W/cm²). $p_r = 2\sqrt{4U_p}$ corresponds to the parallel emission of two electrons with the maximum energy that can classically be acquired in the photon field ($2U_p$).

How does the ion receive its momentum? In the direction transverse to the electric field, the ionic momentum is solely a result of electron-ion interaction during the ionization process. This could be, for example, a scattering of the electrons at the core or a reminiscence of the initial state momentum distribution. Figures 3d–3f show that this transverse momentum distribution becomes wider with increasing peak power. In the rescattering model, this transverse momentum would be mainly a result of the momentum transfer in the $(e, 2e)$ collision. However, the distributions shown in Figs. 3d–3f are about a factor 2–4 narrower than the transverse recoil-ion momentum distribution for double ionization of helium by 270–2000 eV electron impact measured by Jagutzki *et al.* [22].

The component of the momenta parallel to the polarization is mainly a result of the acceleration of the ion in the field. For an estimate, we assume that the first electron is removed at time t_{11} and the ion switches its charge from 1^+ to 2^+ at time t_{12} . If both electrons are removed without momentum transfer to the ion, the ion momentum at the time t_∞ at the end of the laser pulse with the envelope of the electric field strength $E(t)$ is given by (in atomic units)

$$p_z(t_\infty) = \int_{t_1}^{t_{12}} E(t) \sin(\omega t) dt + 2 \int_{t_{12}}^{t_\infty} E(t) \sin(\omega t) dt. \quad (1)$$

For the TS1/shake process, one might assume $\omega(t_{11} - t_{12}) \ll \pi$, i.e., if the double ionization takes place in a time interval short compared to the optical cycle. Then Eq. (1) describes the motion of a particle with charge 2^+ in the oscillating field. The final momentum depends on the phase ωt_1 at the instant of creation of the ion. The maximum value of $2\sqrt{4U_p}$ [shown by the full arrows in Figs. 3(a)–3(c)] corresponds to the creation of the ion when the optical field strength is zero. The data show clearly that the He^{2+} ion yield is strongly suppressed in the region approaching $2\sqrt{4U_p}$. The width of the peak in Fig. 3c corresponds to $\pm 1/4$ field period centered around the maximum field strength. This is consistent with prediction of a time dependent calculation of the He^{2+} yield of Parker and co-workers [23].

Contrary to the shakeoff/TS1 process, in the rescattering model there is a significant time delay between the

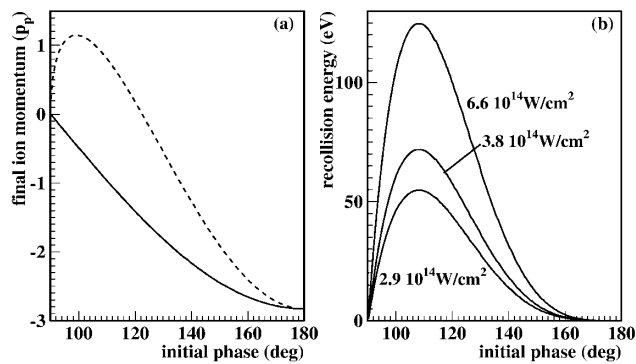


FIG. 4. (a) Final momentum of He²⁺ ion [$p_z^{\text{He}^{2+}}(t_\infty)$] according to Eq. (1) as function of the phase ωt_1 of the laser field at the release of the first electron. The momentum is in units corresponding to the ponderomotive energy $p_p = \sqrt{2U_p}$. The maximum value of 1.15 is shown by the dashed arrows in Fig. 3. The full line is for simultaneous release of both electrons ($t_1 = t_{12}$). The dashed curve corresponds to the rescattering model where t_{12} is the time of the recollision. It does not include momentum transfer during the ($e, 2e$) collision. (b) Electron energy at time of recollision as a function of the initial phase (for 800 nm). The minimum energy for excitation of the He¹⁺ is 40.5 eV.

liberation of the first electron and its reencounter with the ion which leads to double ionization. Figure 4 shows the He²⁺ final state momentum according to Eq. (1) as a function of the initial phase at the instant of single ionization. The dotted line corresponds to t_{12} being the time when the electron reencounters the ion for the first time. Phases smaller than 90° are not shown since they do not lead to return of the electron. Figure 4b shows the energy of the electron at its reencounter (see [3,8]). Double ionization is possible only if the electron has enough energy to at least excite the He¹⁺ ion (40.5 eV). In the rescattering model, the momentum transfer during the ($e, 2e$) collision has to be added to the momenta shown in Fig. 4a. A region for the total momentum including the collisional momenta (see [22]) is shown in Figs. 3a–3c by the hashed area.

In conclusion, our measured He²⁺ momentum distributions are in the direction perpendicular to the light polarization narrower than expected from the rescattering model, and in the parallel direction they evolve into a two peak structure with increasing field strength. Clearly, a more detailed understanding requires theoretical approaches which treat the three-body problem in strong fields (see, e.g., [20,23,24]) and provide information on the correlated motion of all three particles.

We are indebted to Horst Schmidt-Böcking for enthusiastic support of this project and Robert Moshhammer and Joachim Ullrich for many helpful discussions. We thank Andreas Becker for pushing us for many years to perform the experiment reported here and for providing us with calculated ion yields. We profited from discussions on the subject with Lew Cocke, Mike Prior, and Jan Michael Rost. This work is supported by DFG, BMBF, GSI, and DAAD. The Marburg group thanks the DFG for support through their SFB383 and their Graduiertenkolleg “Op-

toelektronik mesoskopischer Halbleiter.” We are grateful to W.W. Rühle for continuous support and valuable discussions.

*Email address: doerner@hsb.uni-frankfurt.de

- [1] D.N. Fittinghoff, P.R. Bolton, B. Chang, and K.C. Kulander, Phys. Rev. Lett. **69**, 2642 (1992).
- [2] B. Walker, B. Sheehy, L.F. DiMauro, P. Agostini, K.J. Schafer, and K.C. Kulander, Phys. Rev. Lett. **73**, 1227 (1994).
- [3] P.B. Corkum, Phys. Rev. Lett. **71**, 1994 (1993).
- [4] J.B. Watson, A. Sanpera, D.G. Lappas, P.L. Knight, and K. Burnett, Phys. Rev. Lett. **78**, 1884 (1997).
- [5] A. Becker and F.H.M. Faisal, J. Phys. B **29**, L197 (1996).
- [6] A. Becker and F.H.M. Faisal, J. Phys. B **32**, L335 (1999).
- [7] K.J. LaGattuta and J.S. Cohen, J. Phys. B **31**, 5281 (1998).
- [8] K.C. Kulander, J. Cooper, and K.J. Schafer, Phys. Rev. A **51**, 561 (1995).
- [9] D.N. Fittinghoff, P.R. Bolton, B. Chang, and K.C. Kulander, Phys. Rev. A **49**, 2174 (1994).
- [10] M. Yu. Kuchiev, J. Phys. B **28**, 5093 (1995).
- [11] B. Sheehy, R. Lafon, M. Widmer, B. Walker, L.F. DiMauro, P.A. Agostini, and K.C. Kulander, Phys. Rev. A **58**, 3942 (1998).
- [12] B. Walker, B. Sheehy, K.C. Kulander, and L.F. DiMauro, Phys. Rev. Lett. **77**, 5031 (1996).
- [13] W.C. Liu, J.H. Eberly, S.L. Haan, and R. Grobe, Phys. Rev. Lett. **83**, 520 (1999).
- [14] J. Ullrich, R. Moshhammer, R. Dörner, O. Jagutzki, V. Mergel, H. Schmidt-Böcking, and L. Spielberger, J. Phys. B **30**, 2917 (1997).
- [15] R. Dörner, V. Mergel, O. Jagutzki, L. Spielberger, J. Ullrich, R. Moshhammer, and H. Schmidt-Böcking, Phys. Rep. (to be published).
- [16] J.H. McGuire, N. Berrah, R.J. Bartlett, J.A.R. Samson, J.A. Tanis, C.L. Cocke, and A.S. Schlachter, J. Phys. B **28**, 913 (1995).
- [17] A. Becker and F.H.M. Faisal, Phys. Rev. A **59**, R1742 (1999).
- [18] V. Mergel, R. Dörner, J. Ullrich, O. Jagutzki, S. Lencinas, S. Nüttgens, L. Spielberger, M. Unverzagt, C.L. Cocke, R.E. Olson, M. Schulz, U. Buck, E. Zanger, W. Theisinger, M. Isser, S. Geis, and H. Schmidt-Böcking, Phys. Rev. Lett. **74**, 2200 (1995).
- [19] R. Dörner, H. Bräuning, J.M. Feagin, V. Mergel, O. Jagutzki, L. Spielberger, T. Vogt, H. Khemliche, M.H. Prior, J. Ullrich, C.L. Cocke, and H. Schmidt-Böcking, Phys. Rev. A **57**, 1074 (1998).
- [20] A. Becker and F.H.M. Faisal, Phys. Rev. A **50**, 3256 (1994).
- [21] F. Maulbetsch and J.S. Briggs, J. Phys. B **28**, 551 (1995).
- [22] O. Jagutzki, L. Spielberger, R. Dörner, S. Nüttgens, V. Mergel, H. Schmidt-Böcking, J. Ullrich, R.E. Olson, and U. Buck, Z. Phys. D **36**, 5 (1996).
- [23] J. Parker, K.T. Taylor, C.W. Clark, and S. Blodgett-Ford, J. Phys. B **29**, L33 (1996).
- [24] D. Dundas, K.T. Taylor, J. Parker, and E. Smyth, J. Phys. B **32**, L231 (1999).